Turkish Journal of Electrical Engineering & Computer Sciences

http://journals.tubitak.gov.tr/elektrik/

Research Article

Turk J Elec Eng & Comp Sci
(2022) 30: 1804 – 1820

doi:10.55730/1300-0632.3906

Breast cancer-caps: a breast cancer screening system based on capsule network utilizing the multiview breast thermal infrared images

Devanshu TIWARI[1,*], **Manish DIXIT**[2], **Kamlesh GUPTA**[3]

[1]Department of Computer Science and Engineering, Rajiv Gandhi Proudyogiki Vishwavidyalaya, Bhopal, India
[2]Department of Computer Science and Engineering, Madhav Institute of Technology and Science, Gwalior, India
[3]Department of Information Technology, Rustamji Institute of Technology, BSF Academy, Tekanpur, India

Received: 21.10.2021 • **Accepted/Published Online:** 28.04.2022 • **Final Version:** 22.07.2022

Abstract: This paper proposed an accurate and fully automated breast cancer early screening system called the "Breast Cancer-Caps". The capsule network is used in this approach for the cancer detection in breast utilizing the thermal infrared images for the first time. This capsule network is trained with the help of Dynamic as well as Static breast thermal images dataset consisting of left, right, frontal views along with a new multiview thermal images. These multiview breast thermal images are fabricated by concatenating the conventional left, frontal and right view breast thermal images. The other current and popular deep transfer learning models such as Visual Geometry Group 19 (VGG 19), Residual Network 50 (ResNet50V2) and InceptionV3 network are also trained with the aid of same Static and Dynamic breast thermal images augmented dataset for comparing the performance of these models with the proposed system. The "Breast Cancer-Caps" system tends to delivers the best testing and validation accuracies as compared to their other deep transfer learning models. This proposed system delivers an encouraging testing accuracy of more than 99% utilizing the multiview breast thermal images as input over the Dynamic breast thermal images testing dataset. Whereas the testing accuracies of 95%, 94% and 89% are achieved by the VGG 19, ResNet50V2, InceptionV3 models respectively over the Dynamic breast thermal images testing dataset utilizing the same multiview breast thermal images as input.

Key words: Thermal images, breast cancer, capsule network, ResNet50V2, InceptionV3, VGG 19, Static, Dynamic, multiview

1. Introduction

The most commonly diagnosed cancer in women's all over the world is the breast cancer malignancy. Its early diagnosis followed by the prognosis can be very helpful in enhancing the chances of patient's survival [1]. As per GLOBOCAN data [2], the breast cancer is the fifth most deadly type of cancer surpassing the lung cancer. The GLOBOCAN 2020 is an online database providing worldwide cancer statistics and estimates of incidence and mortality in 185 countries for 36 types of cancer, and for all cancer sites combined. The cancer of breast originates from the interior lining of the milk ducts or lobules in the breast. The cells of breast cancer are the outcome of DNA or RNA mutation [3]. The major reasons for this harmful mutation are the excessive use of chemicals, electromagnetic radiation, viruses, fungi, and mechanical cell-level injury, parasites, heat, water, and food, free radicals, aging of DNA or RNA etc. [4]. One of the most effective way of diagnosing breast cancer is

*Correspondence: devanshu.tiwari28@gmail.com

to perform regular screening either manually by the doctor or employing medical imaging techniques [5]. The various medical imaging techniques such as mammography, histopathology, ultrasound, infrared thermography etc. are often used by the doctors for the diagnosis of breast cancer. The infrared thermography technique is mostly used for performing the regular screening of breast in order to detect any sort of abnormality or lesion. Such regular screening of breasts as a part of normal health checkup is quite imperative for the detection of breast cancer in early stages and thus reducing its mortality rate. Even some research carried out in the past is claiming that the infrared thermography technique is quite capable of detecting breast abnormalities prior to cancer development [6]. At the same time the infrared thermography technique is painless and can be conducted in a contactless manner, which eventually makes it more popular among the female patients all over the world. Whereas the mammography, histopathology, and ultrasound techniques are painful, expensive on the part of patients and also conducted in a noncontactless manner. Therefore, the infrared thermography technique is mostly prescribed by the doctors as a complementary test for doing the early breast cancer screening. In case of cross-validating a suspicious breast thermal images, it is the mammography or histopathology techniques used by the doctors in order to reach a final diagnostic decision [7, 8]. The thermography technique utilizes the concept of capturing the infrared radiation emitted from the skin of breast, which determines bilateral symmetry patterns in normal cases. Any variation in such symmetry patterns will highlights the presence of anomalies or presence of cancer cells [9]. Generally the Static and Dynamic are the two acquisitions protocols used for the recording of breast thermal infrared images [10, 11]. The Dynamic thermal images are obtained during a particular period of time surpassing the cooling step [12], whereas the Static thermal images are taken at any point of time and one per patient at different angles.

The various computer aided diagnosis (CAD) systems based on machine learning and deep learning are developed in the last decade for the automated early detection and screening of various cancer type classification [13]. The existence of these CAD systems are even more important in present time, where the whole world is experiencing an extreme deficiency of physicians as well as medical facilities for the purpose of diagnosis and treatment of patients in real time [14]. A substantial and quality research is carried out during the last two years in order to develop CAD systems for the automated breast cancer detection majorly utilizing the Mammography, Ultrasound, Infrared thermography and other imaging modalities, which could assist the doctors. The current research trend lies in the development of CAD systems based on deep learning and deep transfer learning models for the correct binary classification into breast normal and abnormal cases. Especially thermography is more popular among the doctors for doing the regular annual screening of women breast as a part of normal health checkup. Due to this fact, there is an imperative need to develop more accurate and efficient CAD systems for performing the early screening of breast thermography images into normal or abnormal images. The other contributions of this research study are stated below:

1. This research article presents an accurate fully automated breast cancer screening system based on the capsule network utilizing both the Static and Dynamic thermal images for the first time.

2. This research article presents a novel idea of training the capsule network with the help of a multiview breast thermal images, which can be fabricated by concatenating the conventional left, right and frontal views breast thermal images for the first time. Then experimentation and simulation is done to showcase that these multiview concatenated thermal images tend to deliver better results as compared to the conventional single view thermal images.

3. This research article also presents a brief experimentation utilizing both types of i.e. Static and Dynamic breast thermal images to showcase which acquisition protocol type delivered better results during

training and testing phase.

There are total six sections present in this research study. Initially the basic information regarding the breast cancer disease and its diagnosis utilizing the infrared thermal images along with the role of machine & deep learning for automating this procedure is well presented in the introduction section. Then the literature review section presents some of the major state of the art automated approaches utilizing the infrared breast thermal images for the breast cancer detection and also the grey areas presents in this research domain. The third section is all about illustrating the proposed method including the brief dataset description, preprocessing and augmentation for increasing the number of training samples along with the description and algorithm of the proposed "Breast Cancer-Caps" system based on the capsule network. The next section is the results section, which presents the performance of the proposed system along with the performance of the VGG19, ResNet50, InceptionV3 based systems used for the comparison over the test static and dynamic breast thermal images dataset. The discussion section presents the merits and issues associated with the training as well as testing of the proposed "Breast Cancer-Caps" system using the left, right frontal and multiview breast thermal images. Finally the conclusion section simply presents a brief analysis of the performance of the proposed "Breast Cancer-Caps" over all four views of breast thermal images and some deep insights of this study to be used in the future.

2. Literature review

The machine learning based approaches for the breast cancer detection utilizing the thermal images generally consist of three major stages i.e. segmentation, feature extraction as well as reduction and last classifier training. When it comes to the accurate breast cancer region of interest segmentation, Fuzzy c-means, Otsu's thresholding, level-set methods, the edge based segmentation, k-means, extended hidden Markov model, etc., are used commonly. Then gray level cooccurrence matrices (GLCM) features, gray level run length (GLRL), Haralick, gray level size zone matrix (GLSZN) and neighborhood grey tone difference matrix (NGTDM) methods, etc., [15–17] are used for the purpose of feature extraction. The various popular machine learning classifiers such as support vector machine (SVM), naïve Bayes (NB), random forest (RF), AdaBoost, k-nearest neighbor (kNN), decision tree, least square support vector machine (LSSVM), etc., [18–21] are trained with the aid of extracted features in order to perform accurate classification. The approaches based on these methods tend to deliver 90% to 97% accuracies over the local as well as global datasets of breast thermal images. The majority of existing approaches for the breast cancer detection utilizing the thermal images are based on the conventional machine learning classifiers, whereas the number of approaches based on deep learning and deep transfer learning is far less. This very fact is also proved with the help of a graph 1 presented in Appendix 1, which showcases the comparison among the number of research and review articles published related to the breast cancer classification utilizing the thermal images based on machine learning and deep learning as per IEEE Xplore and PubMed research databases.

The deep learning or deep transfer learning based breast cancer classification consists of only one major stage i.e. tuning and training of convolutional neural networks utilizing the augmented or normal large size breast thermal images datasets. These deep learning based approaches are completely automated as the various convolutional layers consisting of filters tend to perform the segmentation, features extraction and training by themselves. Some of the recent and accurate breast cancer detection approaches utilizing the thermal images have used the MobileNet, InceptionNet, VGG 16, VGG 19, ResNet152, ResNet18, ResNet101, ResNet50, ResNet34, etc. [22–25]. A brief comparison among these state of the art thermography based breast cancer

classification approaches is presented with the aid of Appendix 1. From the literature review above, the following points can be concluded as follows:

1. Deep learning based approaches are fully automated and also tend to be more accurate as compared to the machine learning based approaches. The capsule networks are the evolving and new class of neural networks, which tend to deliver better results in various cancer classification and other computer vision tasks. So there is a need to develop a fully automated capsule network based breast cancer screening system using the thermal infrared images as no such system exists until now. The other reason of using the capsule network is the fact that this class of neural network tends to perform better on the augmented datasets as compared to other deep transfer learning models.

2. The majority of all the abovementioned approaches have only used the frontal view breast thermal images for breast cancer classification. There is no approach proposed yet, which even tried experimentation with the different views of breast thermal images. A breast multiview concatenated thermal image consisting of front, left and right may represent more information and hence proved to be more useful for getting good results.

3. Experimentation is also required to do with respect to the usage of Static and Dynamic thermal images for the training as well as testing purpose just to showcase which of these two thermal acquisition protocols are delivering better results. None of the approaches has done this type of experimentation.

3. Proposed approach

The preprocessing along with augmentation and training of capsule network is the major stages of this proposed approach for the binary breast cancer classification into normal or abnormal cases. The overall proposed approach is well presented with the help of Figure 1 below:

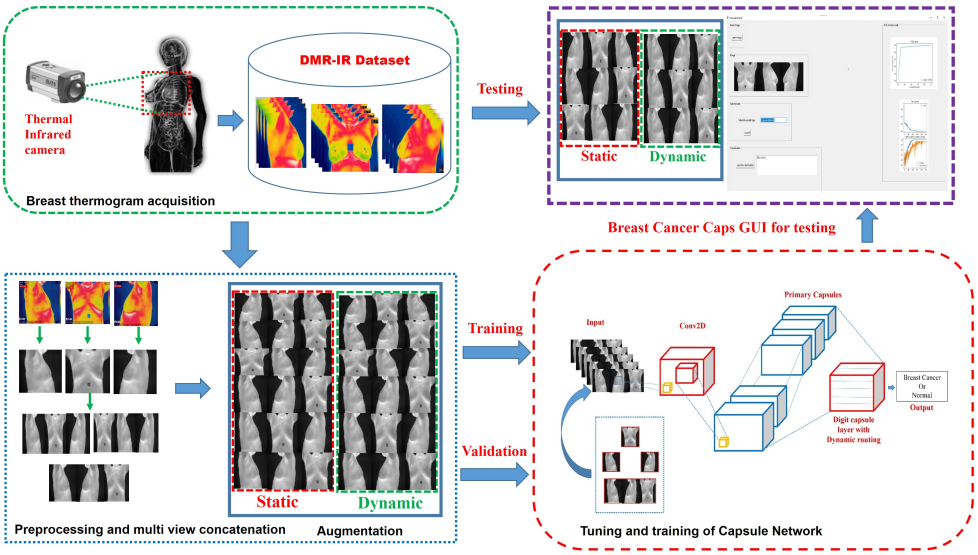

Figure 1. The overall proposed approach based on the capsule network utilizing the multiview breast thermal images for the breast cancer detection.

3.1. Dataset description

The DMR-IR dataset [16] is used in this research study[1]. This is the only database available for the breast thermal images consisting of images acquired using both the Static and Dynamic protocol. In this database, breast thermal images of 287 women volunteers are present. These thermal images are acquired with the aid of thermal camera i.e. FLIR SC-620 at resolution of 640 × 480 with thermal sensitivity of 40 mk (at 20 °C). For this study and in order to cover the entire breast region, we have taken per patient three lateral views i.e. left, frontal and right of Static as well as Dynamic thermal images of 150 subjects for training purposes. Out of these 150 subjects in which 80 are unhealthy and 70 are healthy subjects. Hence the training Static breast thermal images dataset consist of total 600 concatenated multiview, left, right and frontal views thermal images of both the healthy and unhealthy subjects. Whereas the training Dynamic breast thermal images dataset consist of total 600 concatenated multiview, left, right and frontal views thermal images of the healthy and unhealthy subjects. For the testing purpose, Static and Dynamic testing dataset consist of thermal images of 50 subjects in which 25 are diagnosed as healthy and remaining 25 are diagnosed as unhealthy subjects (having breast cancer). The Static testing dataset consist of 50 multiview, 50 left, 50 right and 50 frontal view breast thermal images of both the healthy and unhealthy subjects. Similarly, the Dynamic testing dataset consist of 50 multiview, 50 left, 50 right and 50 frontal view breast thermal images of both the healthy and unhealthy subjects.

3.2. Preprocessing and augmentation

Initially, both Static and Dynamic thermal images undergo cropping, contrast enhancement, normalization and lastly resizing as preprocessing steps. Then multiview breast thermal images are generated by initially concatenating the left, frontal and right views with the aid of hconcat() function used for the horizontal concatenation and vconcat() function used for the vertical concatenation available in the libraries of the OpenCv and NumPy in Python. These images are transformed into the thermal images of dimension 480 × 120, as this size as input offered the best accuracy quotient with least training time. Now both these preprocessed Static and Dynamic datasets are augmented with the help of the ImageDataGenerator function of Keras. These two datasets now underwent augmentation utilizing data generation of 4 types like rotation range, shear range, rescaling and zoom range [26, 27]. After doing a number of experiments, the best values for rotation range = 5, shear range = 0.02, zoom range = 0.02 and rescale = 1./255. The augmentation is done in order to have a large size dataset of infrared breast thermal images, so the capsule network model trains perfectly and the problem of over fitting is avoided.

3.3. Capsule network

Primarily the capsule network consist of capsules and in turn these capsules are the clusters of neurons [28]. The different instantiation parameters of the concerned entity are represented by the activity vectors of the neurons of a capsule. Whereas the probability that a spatial entity exists is denoted by the length of these vectors. In conventional neural network, the pooling layers are held responsible for most of the deficiencies. The performance issues related to pooling's layers are overcome with the aid of routing by agreement principle used in the capsule network [29]. The first layer generated output are send to the next layer consisting of parental level capsules in this routing by agreement principle, as all the capsules attempts to classify the parental capsules'

[1] http://visual.ic.uff.br/dmi

outputs with even different capsules' coupling coefficient [30]. An increase in the coupling coefficient of the related capsules is caused due to the anticipated conformations of the parent capsules objectified outputs. As the capsule x is l_x therefore its exposure for the y parent capsule is computed employing the formula illustrated with the help of Equation 1 as:

$$l^{'}{}_{y|x} = O_{xy} l_x. \tag{1}$$

The $l_{y|x}$ simply represents the y^{th} higher layer capsule anticipated vector of its output as compared in the preceeding layers by the x capsule. The O_{xy} is the coefficient weighted matrix as a result of regressive process. The h_{xy} as the coupling coefficeint, which totally depends on the amount of conformations of the parent capsules as well as the beneath layers. This h_{xy} is represented with the aid of Equation 2:

$$h_{xy} = \exp(g_{xy}) / \sum_{z} \exp(g_{xz}). \tag{2}$$

At the beginning of the process, the g_{xy} is equal to zero and its simply represents the probability of log for determining, if capsule y is coupled to capsule x or not. So the q_y parent capsule input vector is well defined with the aid of Equation 3 as:

$$q_y = \sum_{x} h_{xy} l^{'}{}_{y|x}. \tag{3}$$

Equation 4 simply defined that the initial vector can be employed to get the final output of each capsule. This equation also makes sure that capsules output never go above 1 value.

$$m_y = ||q_y||^2 \; q_y \; / (1 + ||q_y||^2) \; ||q_y|. \tag{4}$$

The y's capsule output as well as the input vector are denoted by the terms q_y and m_y. Since the probability of log updates in innumerable in this routing process. Which also means that the large inner product is produced due to the agreements between m_y and $l_(y|x)$ exploiting the realities of the two supportive vectors. Finally, Equation 5 represents the coupling coefficients as well as the m_{xy} agreement for amending the log probability.

$$f_{xy} = \; m_y . \; l^{'}{}_{y|x} \tag{5}$$

The loss function is computed with the aid of Equation 6 below. It is a function that intends to give high loss value on capsules processing parameters of long output instigation types especially when the entity existence is not recorded.

$$t_z = R_z \; max \; \left(0, \; m^+ - ||m_z||\right)^2 + \delta(1 - \; R_z) \max(0, ||m_z|| - \quad m^-)^2 \tag{6}$$

Whenever k class exist, the value of R_z is 1 otherwise 0. Since important parameters such as δ, m^-, m^+ are prior established, the learning procedure starts.

3.3.1. The proposed capsule network architecture

The architecture of our proposed capsule network for the breast cancer detection simply consist of four layers along with an input layer, which takes a breast thermal images image of dimension 480 × 120. Then followed by a convolutional layer (Conv2D) consisting of "Relu" activation function and 256 filters in order to extract the primary feature maps. In this layer, every capsule consists of kernel size of 9 with stride value two. The next

layer is the primary capsule layer, which divides the features maps into capsules. In this layer, a weight matrix of size 8×16 is multiplied to each capsule after convolution. Finally, the operations of squashing and dynamic routing are applied to each capsules in the digitacaps layer [31]. This layer is an auxiliary layer to replace each capsule with its length and is used for performing the correct classification and delivers output as the normal or abnormal breast. The architecture of the proposed capsule network for breast cancer screening is illustrated with the help of Figure 2. The model summary of the proposed capsule network for breast cancer screening is illustrated with the help of Appendix 2. The algorithm of the proposed "Breast Cancer-Caps" based on capsule network is given below as proposed breast cancer-caps algorithm:

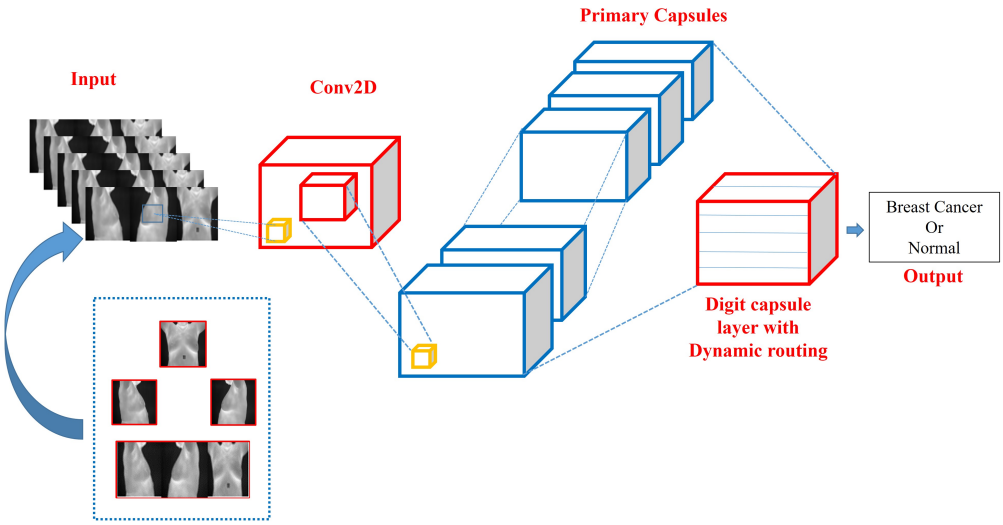

Figure 2. The proposed capsule network architecture for the breast cancer screening.

3.4. Comparison approach

The VGG19 [32], ResNet50 [33] and InceptionV3 [34] deep transfer learning (DTL) models are employed for the purpose of comparison and evaluation on both the datasets i.e. Static and Dynamic breast thermal images datasets. Initially, three models are properly fine-tuned and trained using the same Static and Dynamic breast thermal images augmented datasets. The objective of this comparison is to present the fact that how efficiently these popular and complex DTL models perform on the abovementioned datasets in comparison with the capsule network. The VGG19, ResNet50V2 and InceptionV3 DTL models hyperparameters values are chosen based on a experimental method [35] offering the best performance and presented with the help of Table 1. The Adam [36] as an optimizer technique is used for weight adjustment along with the 0.00001 learning rate and mini batch size of 16 for all the three DTL models. The overall algorithm for the comparison approach is given below as comparison approach algorithm:

4. Results

The Python 3.6 is used as an implementation programming language along with the Google Colaboratory (colab) platform is used for the experimentation and simulation in this research study. This result section consists of two subsections. The first section illustrates the performance of the proposed "Breast Cancer-Caps" system

Algorithm 1 Proposed breast cancer-caps algorithm.

Input:

1. Augmented Dynamic breast thermal images dataset consists of normal and abnormal images
2. Augmented Static breast thermal images dataset consists of normal and abnormal images

Output: The Fine-tuned and trained capsule network as the "Breast Cancer-Caps"

Procedure:

1: Preprocess the breast thermal images taken from the DMR-IR database in order to remove the noise, symbols and artifacts and develop two datasets i.e. Static and dynamic breast thermal images datasets.

2: Then generate a multiview breast thermal image by concatenating the conventional frontal, left and right breast region views in both these Static and Dynamic breast thermal images datasets using the hconcat() and vconcat() functions available in the OpenCV and NumPy libraries.

3: Then perform the augmentation of both these datasets using the Keras ImageDataGenerator function of four types i.e. rotation range = 5, shear range = 0.02, zoom range = 0.02 and rescale = 1./255.

4: These augmented datasets images are resized to respective dimensions of 480 × 120 for the capsule network. As the capsule network is based on the routing by agreement principle and its step by step procedure as under:

Routing_CapsNet ($l'_{y|x}$, I, n)

I Initialize log prior probabilities (logit) of all capsules in a layer (x) and above layer (y) for all capsule x in layer n and capsule y in layer n+1: $g_{xy} \leftarrow 0$.

II Repeat steps III to VI for i^{th} times.

III Compute softmax function i.e. how capsule (x) of layer (n) is coupled to capsule above layer (n+1) for all capsule x in layer n: softmax (g_x)

IV Compute input to a capsule (y) in just above layer (n+1)
for all capsule y in layer n+1: $q_y = \sum_x h_{xy} l'_{y|x}$

V Compute output of a capsule (y) in just above layer (n+1) using squash function
for all capsule y in layer n+1: $m_y = ||q_y||^2 \; q_y \; /(1+||q_y||^2) \; ||q_y||$

VI Update initial log it for next iteration
for all capsule x in layer n and capsule y in layer n+1: $g_{xy} \leftarrow g_{xy} + m_y . \; l'_{y|x}$

VII Return output of the capsule y Return m_y

5: The capsule network tends to converge at 500 epochs as the training loss remains constant after this.

using various performance evaluation metrics utilizing the single views as well as multiview breast thermal images. As the two i.e. Static and Dynamic testing datasets are prior developed from the DMR-IR database and consist of breast thermal images of multiview, left, right and frontal view of 25 breast cancer patients as unhealthy subjects and 25 healthy subjects. The accuracy, sensitivity, specificity, precision, F1 score, mean square error [37], cross entropy loss [38], area under the receiver operating characteristic curve (ROC-AUC) [39, 40] and Kappa coefficients [41] are the performance evaluation metrics used. The performance of the proposed "Breast Cancer-Caps" system over both the Static and Dynamic testing datasets are presented with the help of Table 2. The testing procedure is repeated five times and the mean values of the performance evaluation metrics are presented in Table 2. Whereas the best confusion metrics obtained during this testing

Table 1. The VGG19, InceptionV3 and ResNet50V2 hyperparameters values.

DTL models parameters	VGG19	InceptionV3	ResNet50
Input image size	224 × 224	299 × 299	224 × 224
Number of layers	19	48	50
Learning rate	0.00001	0.00001	0.00001
Batch size	16	16	16
Number of epochs for training	500	500	500
Momentum	0.9	0.9	0.9
Optimizer	Adam	Adam	Adam

Algorithm 2 Comparison approach algorithm.

Input:

1. Augmented Dynamic breast thermal images dataset consists of normal and abnormal images
2. Augmented Static breast thermal images dataset consists of normal and abnormal images

Output: The fine-tuned and trained VGG 19, ResNet50 and InceptionV3 models for breast cancer screening

Procedure:

1: Preprocess the breast thermal images taken from the DMR-IR database in order to remove the noise, symbols and artifacts and form two datasets i.e. Static and Dynamic breast thermal images datasets.
2: Then generate a multiview breast thermal images by concatenating the conventional frontal, left and right breast views in both these Static and Dynamic breast thermal images datasets.
3: Then perform the augmentation of both these datasets using the Keras ImageDataGenerator function of four types i.e. rotation range = 5, shear range = 0.02, zoom range = 0.02 and rescale = 1./255.
4: These augmented datasets images are resize to respective dimensions of 224 × 224 for the VGG 19, ResNet50V2 and dimension of 299 × 299 for the InceptionV3 DTL models.
5: The fine tuning and training of three DTL models are done over both the augmented datasets.
6: The VGG19 models tend to converge at 100 epochs but trained till 500 epochs.
7: Whereas, the ResNet50 and InceptionV3 tend to converge at 200 epochs but trained till 500 epochs.

phase over the Static and Dynamic breast thermal testing datasets are presented in Appendix 3. The proposed "Breast Cancer-Caps" system is delivering 100% training accuracy over the 70% augmented dataset and more than 96% validation accuracy over the remaining 30% augmented dataset. The ROC curve obtained over the validation testing dataset as well as the graph depicting the training loss and training & validation accuracy graph of the proposed "Breast Cancer-Caps" system over both the Static and Dynamic training datasets are presented with the help of Figure 3 below.

The performance of the VGG 19, ResNet 50V2 and InceptionV3 DTL models over both the Static and Dynamic testing datasets are presented with the help of Tables 3–5. Whereas the ROC curve over the validation testing dataset, training loss graph and training & validation accuracy graph of these DTL models over both the training datasets are illustrated with the help of Figures 4–6. Apart from this, performance comparison of the proposed "Breast Cancer-Caps" system with the some of the existing state of the art approaches for the breast cancer classification over the Static and Dynamic testing datasets are also presented in Appendix 3. The performance of the proposed "Breast Cancer-Caps" system is much superior as compare to the performance of these three DTL models and the existing state of the art approaches.The GUI screenshot of the working "Breast

Table 2. The performance of the proposed "Breast Cancer-Caps" over the Static and Dynamic testing datasets.

Performance evaluation metrics	Multiview breast thermal image		Left view breast thermal image		Right view breast thermal image		Frontal view breast thermal image	
	Static	Dynamic	Static	Dynamic	Static	Dynamic	Static	Dynamic
Accuracy	98	99.5	83	85	87	87	93	94
Sensitivity	98	98.04	82.35	84.31	87.76	86.27	95.74	95.83
Specificity	98	100	83.67	85.71	86.27	87.76	90.57	92.31
Precision	98	100	84	86	86	88	90	92
F1 score	98	99.01	83.17	85.15	86.87	87.13	92.78	93.88
Mean square error	0.021	0.019	0.178	0.174	0.151	0.150	0.071	0.070
Cross entropy loss	0.086	0.084	0.66	0.64	0.340	0.338	0.451	0.448
AUC	98.2	99.1	90.5	91.4	92.5	92.7	96.5	97.1
Kappa coefficient	0.96	1	0.68	0.72	0.72	0.73	0.88	0.88

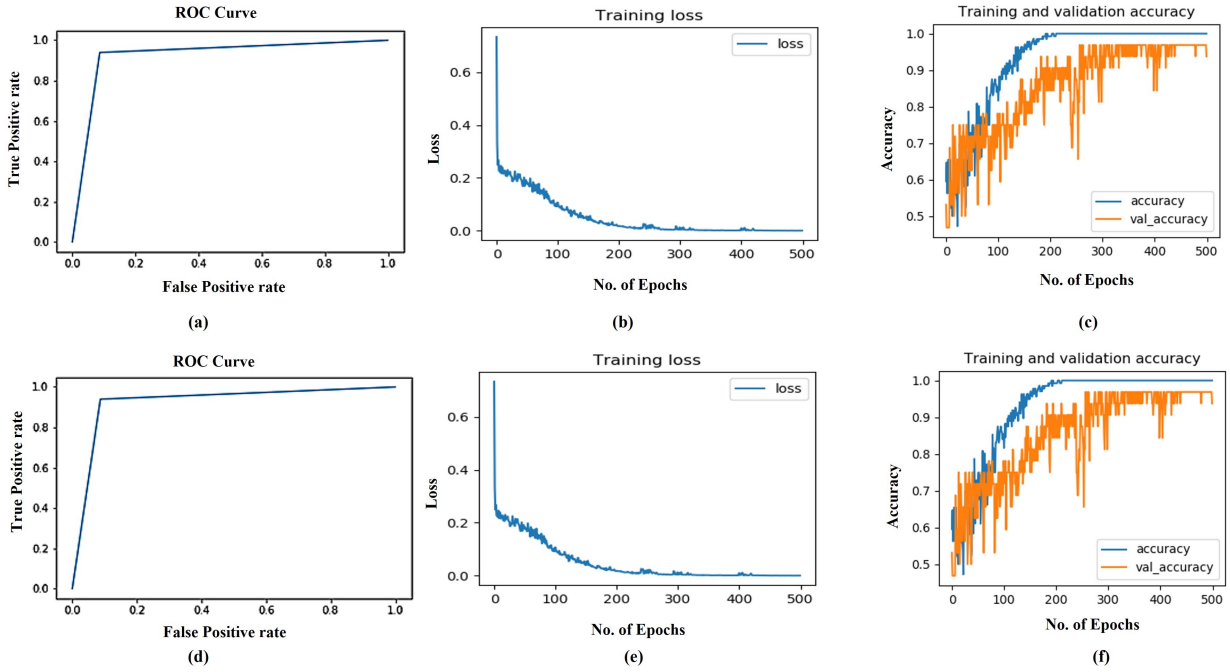

Figure 3. The ROC curve, training loss and training & validation accuracy graph of the proposed "Breast Cancer-Caps" over the Static breast thermal images dataset is represented by a, b, c and over the Dynamic breast thermal images dataset is represented by d, e, f.

Cancer-Caps" system is illustrated with the help of Appendix 3.

5. Discussion

The proposed "Breast Cancer-Caps" system based on the capsule network is proved to be very accurate especially in terms of performing the binary classification of breast cancer thermal images as compared to other deep transfer learning models. The major reason of employing the capsule network is its ability to deal with affine transformations and noise, which are very common in the breast infrared thermal images. Initially, the breast

Table 3. The performance of the VGG19 DTL model over Static and Dynamic testing datasets.

Performance evaluation metrics	Multiview breast thermal image		Left view breast thermal image		Right view breast thermal image		Frontal view breast thermal image	
	Static	Dynamic	Static	Dynamic	Static	Dynamic	Static	Dynamic
Accuracy	95	96	82	83	86	88	89	90
Sensitivity	94.12	96	83.3	83.67	89.13	91.3	91.4	91.67
Specificity	95.92	96	80.7	82.35	83.3	85.19	86.7	88.46
Precision	96	96	80	82	82	84	86	88
F1 score	95.05	96	81.6	82.8	85.4	87.5	88.6	89.8
Mean square error	0.071	0.069	0.181	0.178	0.174	0.150	0.148	0.147
Cross entropy loss	0.152	0.149	0.68	0.66	0.64	0.438	0.438	0.418
AUC	96.7	97.4	89.5	90.5	91.4	92.7	92.7	92.8
Kappa coefficient	0.96	0.96	0.64	0.64	0.68	0.75	0.76	0.8

Table 4. The performance of the ResNet 50V2 DTL model over Static and Dynamic testing datasets.

Performance evaluation metrics	Multiview breast thermal image		Left view breast thermal image		Right view breast thermal image		Frontal view breast thermal image	
	Static	Dynamic	Static	Dynamic	Static	Dynamic	Static	Dynamic
Accuracy	94	95	81	82	82	83	90	91
Sensitivity	94	94.12	80.39	82	83.3	83.67	95.4	93.6
Specificity	94	95.9	81.6	82	80.7	82.35	85.7	88.68
Precision	94	96	82	82	80	82	84	88
F1 score	94	95.05	81.19	82	81.6	82.8	89.39	90.7
Mean square error	0.070	0.068	0.184	0.181	0.181	0.178	0.147	0.145
Cross entropy loss	0.148	0.146	0.69	0.68	0.68	0.66	0.518	0.511
AUC	97.1	97.7	89.9	89.5	90.2	90.5	92.8	92.9
Kappa coefficient	0.88	0.96	0.61	0.64	0.62	0.64	0.80	0.82

Table 5. The performance of the InceptionV3 DTL model over Static and Dynamic testing datasets.

Performance evaluation metrics	Multiview breast thermal image		Left view breast thermal image		Right view breast thermal image		Frontal view breast thermal image	
	Static	Dynamic	Static	Dynamic	Static	Dynamic	Static	Dynamic
Accuracy	89	91	80	82	81	83	84	85
Sensitivity	89.8	91.8	82.6	84.78	82.98	86.67	88.6	88.8
Specificity	88.24	90.2	77.7	79.63	79.2	80	80.36	81.8
Precision	88	90	76	78	78	78	78	80
F1 score	88.9	90.9	79.17	81.25	80.41	82.1	82.9	84.21
Mean square error	0.148	0.145	0.187	0.179	0.184	0.178	0.175	0.174
Cross entropy loss	0.438	0.411	0.695	0.67	0.69	0.66	0.64	0.64
AUC	92.7	92.9	89.2	90.1	89.9	90.5	90.8	91.4
Kappa coefficient	0.76	0.82	0.6	0.64	0.61	0.64	0.65	0.65

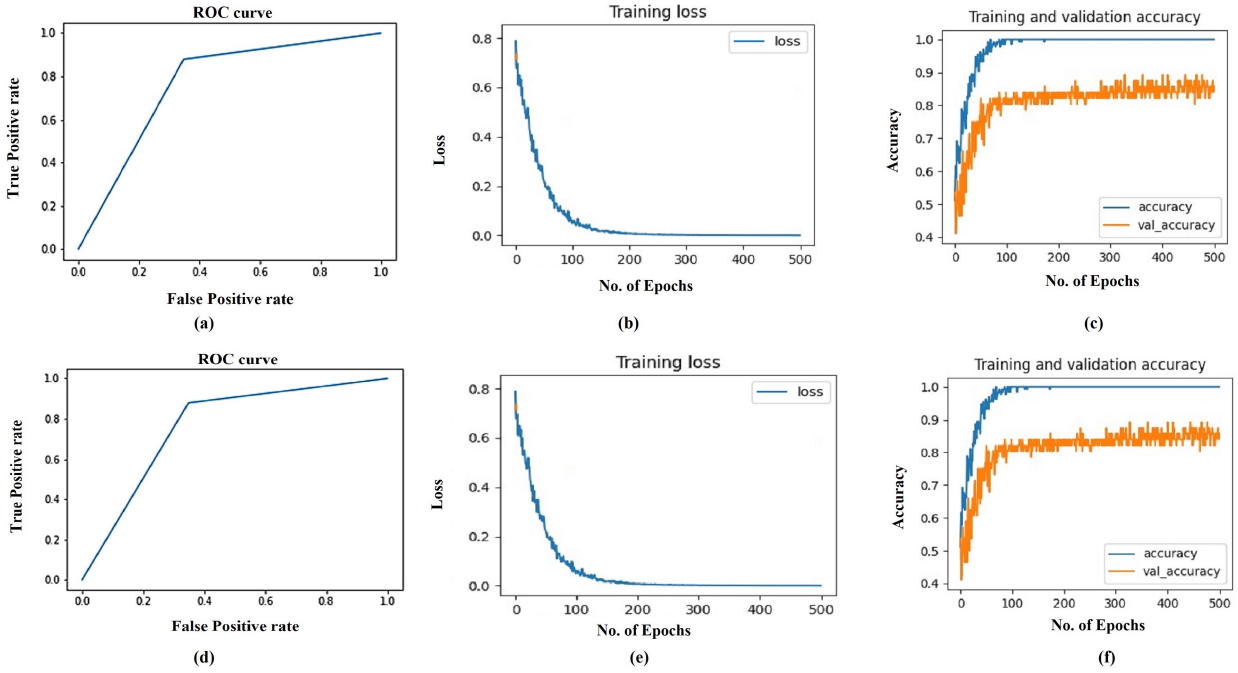

Figure 4. The ROC curve, training loss and training & validation accuracy graph of the comparison approach based on VGG19 model over the Static breast thermal images dataset is represented by a, b, c and over the Dynamic breast thermal images dataset is represented by d, e, f.

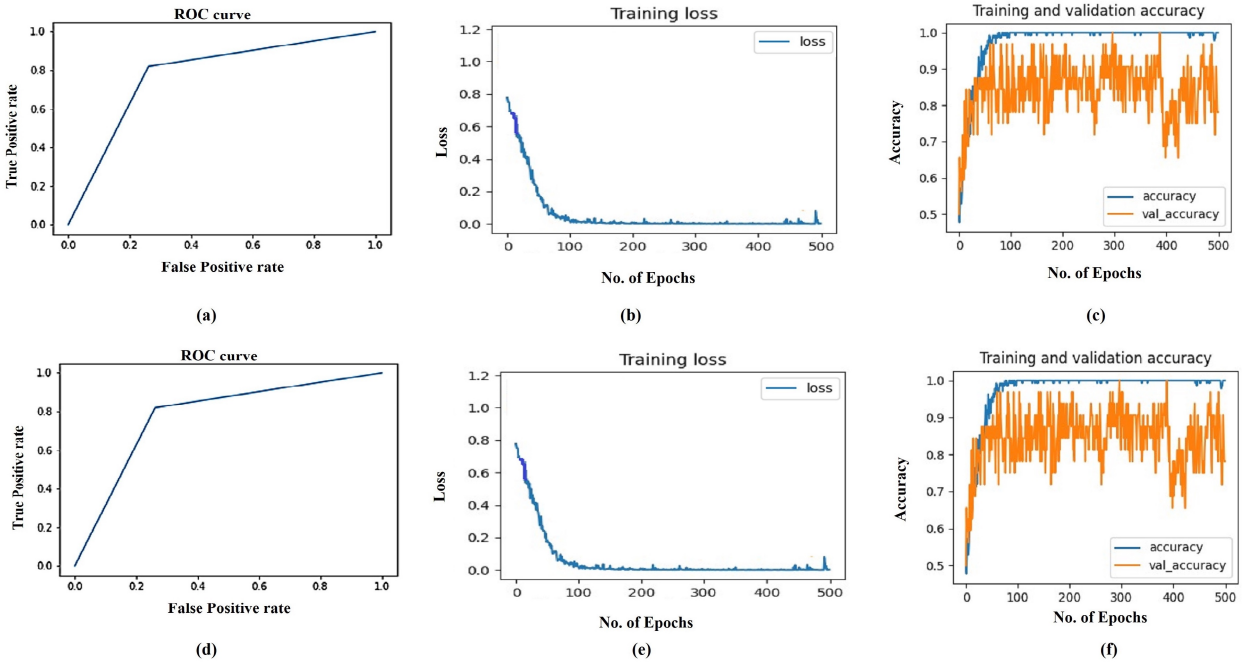

Figure 5. The ROC curve, training loss and training & validation accuracy graph of the comparison approach based on ResNet50V2 model over the Static breast thermal images dataset is represented by a, b, c and over the Dynamic breast thermal images dataset is represented by d, e, f.

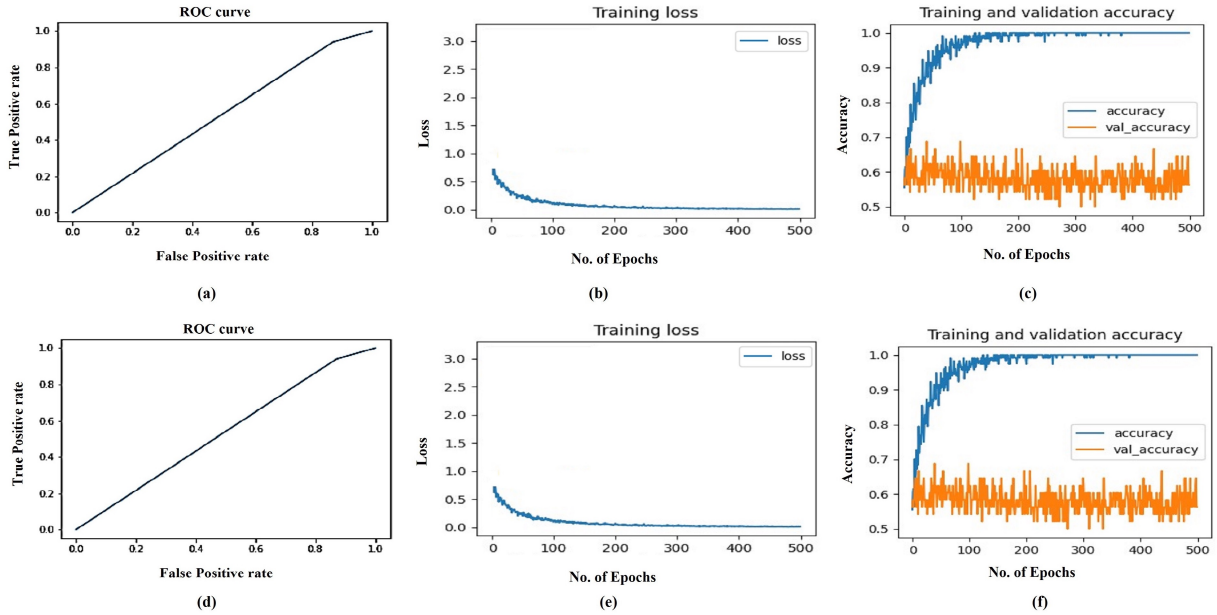

Figure 6. The ROC curve, training loss and training & validation accuracy graph of the comparison approach based on InceptionV3 model over the Static breast thermal images dataset is represented by a, b, c and over the Dynamic breast thermal images dataset is represented by d, e, f.

thermal image of different sizes are tried as input in order to find the best size that offers the least training time while offering the best accuracy quotient. The proposed capsule network based model offers the highest training time with input size as 512 × 512, whereas the proposed model offers the best accuracy quotient with least training time with input of 480 × 120 size breast thermal images. So this input size is used in the research study for training and testing the "Breast Cancer-Caps" system. The other input sizes that are used in the experimentation are 512 × 480, 480 × 480, 480 × 240, 480 × 60, etc. The performance comparison along with the more complex deep transfer learning models in the result section simply proves that the capsule network based system is more robust and accurate. The parameters associated with the capsule network for the proper tuning are decided after performing a number of experiments. The capsule network tends to converge at 500 epochs during training, whereas the other three DTL models tends to converge much earlier during training at either 100 or 200 epochs. Apart from the fact that the capsule network are taking more time to converge, there is no other drawbacks, which can be associated with this proposed system. As the doctors are more inclined towards using the breast frontal view for the correct diagnosis as compared to the left and right view. So we have decided to utilize all the three views along with the newly concatenated multiview breast thermal for performing the experimentation in this research study.

Remarks: Some of the major insights of the main result are as follows:

1. Multiview breast thermal images are more useful for getting reliable and accurate results in comparison to the single view images in this research domain. So 3D breast thermal images can be generated and used in future for better classification accuracy.

2. Multiview thermal images with resolution 480 × 120 is the most appropriate for the training and testing of this capsule network based "Breast Cancer-Caps" system. As with this resolution, the proposed systems offer least training time without compromising on the classification accuracy quotient.

3. The Dynamic acquisition protocol based breast thermal images are far better in comparison to the

static protocol based breast thermal images in terms of delivering better performance for the breast cancer or abnormality detection.

6. Conclusion

This proposed "Breast Cancer-Caps" system based on the capsule network is the first approach, which has utilized the concept of multiview breast thermal images for the detection of breast cancer abnormality. In this research study, the concatenated multiview breast thermal images tend to deliver high accuracy in comparison with conventional single views breast thermal images as these multiview images offer more information to the proposed "Breast Cancer-Caps" system. So the concept of multiview breast thermal images could also be used along with other new and complex deep learning neural networks, which might offers better results in future. This "Breast Cancer-Caps" system tends to delivers better results with the help of Dynamic multiview as well as single view breast thermal images in comparison to the Static breast thermal images. So Dynamic breast thermal images are proved to be more effective for the correct detection of breast cancer abnormality in general.

It is the single view frontal breast thermal images after the concatenated multiview breast thermal images, which delivers satisfactory results. The single view left and right breast thermal images are not that much effective for the detection of breast cancer abnormality as they both offer least testing accuracies values. The proposed "Breast Cancer-Caps" system tends to outperform the three deep transfer learning models i.e. VGG19, ResNet50V2 and InceptionV3. These DTL models are very popular and also deliver good results in other medical imaging classification tasks. The proposed "Breast Cancer-Caps" system achieves testing accuracies of 99.5% and 98% with concatenated multiview Dynamic as well as Static breast thermal images. The fact that capsule networks perform better in comparison to other conventional neural networks especially over the augmented datasets is well established and proved in this research study. Capsule network based "Breast Cancer-Caps" systems perform better in comparison with popular deep transfer learning models such as ResNet50V2, InceptionV3 and VGG19.

The future work involves the development of single view as well as multiview large size breast thermal images dataset along with the clinical information of each women volunteer, so this clinical information can also be taken into account for the breast cancer accurate classification. Apart from this, the quotient of utilizing this multiview breast thermal images could be used in future along with other advanced 3D CNN networks as well DTL models for further enhancing the accuracy and robustness. A set up consisting of thermal cameras along with the proposed "Breast Cancer-Caps" system can be installed in the hospitals for performing the regular screening of women breast in order to diagnose any type of breast cancer abnormality and hence can play an important role in providing proper healthcare.

References

[1] Duffy SW, Tabár L, Yen AM, Dean PB, Smith RA et al. Benecial Effect of Consecutive Screening Mammography Examinations on Mortality from Breast Cancer: A Prospective Study. Radiology 2021; 299 (3): 541-547. doi:10.1148/radiol.2021203935

[2] Sung H, Ferlay J, Siegel RL, Laversanne M, Soerjomataram I et al. Global Cancer Statistics 2020: GLOBOCAN Estimates of Incidence and Mortality Worldwide for 36 Cancers in 185 Countries. CA a cancer journal of clincians 2021; 71 (3): 209-249. doi: 10.3322/caac.21660

[3] Xu X, Yuan X, Ni Jiali, Guo J, Gao Y et al. MAGI2-AS3 inhibits Breast cancer by downregulating DNA methylation of MAGI2. Journal of Cellular Physiology 2021; 236 (2): 1116-1130. doi: 10.1002/jcp.29922

[4] Jahan N, Jones C, Rahman RL. Endocrine prevention of Breast cancer. Molecular and Cellular Endocrinology 2021; 530: 111284. doi: 10.1016/j.mce.2021.111284

[5] Allweis TM, Hermann N, Berenstein-Molho R, Guindy M. Personalized Screening for Breast Cancer: Rationale, Present Practices, and Future Directions. Annals of surgical oncology 2021; 28 (8): 4306-4317. doi: 10.1245/s10434-020-09426-1

[6] Lozano A, Hassanipour F. Infrared imaging for Breast cancer detection: An objective review of foundational studies and its proper role in Breast cancer screening. Infrared Physics & Technology 2019; 97: 244-257. doi: 10.1016/j.infrared.2018.12.017

[7] Gogoi UR, Majumdar G, Bhowmik MK, Ghosh AK. Evaluating the Efficiency of Infrared Breast Thermography for Early Breast Cancer Risk Prediction in Asymptomatic Population. Infrared Physics & Technology 2019; 99: 201-211. doi: 10.1016/j.infrared.2019.01.004

[8] Ter-Minassian M, Schaeffer ML, Jefferson CR, Shapiro SC, Suwannarat P et al. Screening and Preventative Strategies for Patients at High Risk for Breast Cancer. JCO Oncology Practice 2021; 17 (4) : e575-e581. doi: 10.1200/OP.20.00262

[9] Yao X, Wei W, Li J, Wang L, Xu Z et al. A comparison of mammography, ultrasonography, and far-infrared thermography with pathological results in screening and early diagnosis of Breast cancer. Asian Biomedicine 2014; 8 (1): 11–19. doi: 10.5372/1905-7415.0801.257

[10] Hakim A, Awale RN. Thermal Imaging - An Emerging Modality for Breast Cancer Detection: A Comprehensive Review. Journal of Medical Systems 2020;44 (8):136. doi: 10.1007/s10916-020-01581-y

[11] Mambou SJ, Maresova P, Krejcar O, Selamat A, Kuca K. Breast Cancer Detection Using Infrared thermal Imaging and a Deep Learning Model. Sensors 2018; 18 (9): 2799. doi: 10.3390/s18092799

[12] Zuluaga-Gomez J, Al Masry Z, Benaggoune K, Meraghni S, Zerhouni N. A CNN-based methodology for Breast cancer diagnosis using thermal images. Computer Methods in Biomechanics and Biomedical Engineering: Imaging & Visualization 2020; 9 (2): 131–145. doi: 10.1080/21681163.2020.1824685

[13] González FJ, González R, López JC. Thermal contrast of active dynamic thermography versus Static thermography. Biomedical Spectroscopy and Imaging 2019; 8 (1-2): 41–45. doi: 10.3233/BSI-190188

[14] Roslidar R, Rahman A, Muharar R, Syahputra MR, Arnia F et al. A Review on Recent Progress in thermal Imaging and Deep Learning Approaches for Breast Cancer Detection. IEEE Access 2020; 8: 116176-116194. doi: 10.1109/ACCESS.2020.3004056

[15] Husaini MASA, Habaebi MH, Hameed SA, Islam MR, Gunawan TS. A Systematic Review of Breast Cancer Detection Using Thermography and Neural Networks. IEEE Access 2020; 8: 208922-208937. doi: 10.1109/ACCESS.2020.3038817

[16] Silva L, Saade D, Sequeiros G, Silva AC, Paiva AC et al. A new database for Breast research with infrared image. Journal of Medical Imaging and Health Informatics 2014; 4 (1): 92–100. doi: 10.1166/jmihi.2014.1226

[17] Silva LF, Santos AAS, Bravo RS, Silva AC, Muchaluat-Saade DC et al. Hybrid analysis for indicating patients with Breast cancer using temperature time series. Computer Methods and Programs in Biomedicine 2016; 130: 142–153. doi: 10.1016/j.cmpb.2016.03.002

[18] Lashkari A, Pak F, Firouzmand M. Full Intelligent Cancer Classification of thermal Breast Images to Assist Physician in Clinical Diagnostic Applications. Journal of Medical Signals and Sensors 2016; 6 (1): 12-24.

[19] Raghavendra U, Acharya UR, Ng EYK, Tan JH, Gudigar A. An integrated index for Breast cancer identification using histogram of oriented gradient and kernel locality preserving projection features extracted from thermal images. Quantitative Infrared Thermography Journal 2016; 13: 195-209. doi: 10.1080/17686733.2016.1176734

[20] Santana MA, Pereira JMS, Silva FL, Lima NM, Sousa FN et al. Breast cancer diagnosis based on mammary thermography and extreme learning machines. Research on Biomedical Engineering 2018; 34 (1): 45–53. doi: 10.1590/2446-4740.05217

[21] Madhavi V, Thomas CB. Multi-view Breast thermal images analysis by fusing texture features. Quantitative InfraRed Thermography Journal 2019; 16 (1): 111–128. doi: 10.1080/17686733.2018.1544687

[22] AlFayez F, El-Soud MWA, Gaber T. Thermal images Breast Cancer Detection: A Comparative Study of Two Machine Learning Techniques. Applied Sciences 2020; 10 (2): 551. doi: 10.3390/app10020551

[23] Mishra V, Rath SK. Detection of Breast cancer tumours based on feature reduction and classification of thermal images. Quantitative InfraRed Thermography Journal 2021; 18 (5): 300-313. doi: 10.1080/17686733.2020.1768497

[24] Yadav SS, Jadhav SM. Thermal infrared imaging based Breast cancer diagnosis using machine learning techniques. Multimedia Tools and Applications 2020; 81: 13139–13157. doi: 10.1007/s11042-020-09600-3

[25] Ekici S, Jawzal H. Breast cancer diagnosis using thermography and convolutional neural networks. Medical Hypotheses 2020; 137: 109542. doi: 10.1016/j.mehy.2019.109542

[26] Galván JCT, Guevara E, Machuca EMK, Villanueva AC, Flores JL et al. Deep convolutional neural networks for classifying Breast cancer using infrared thermography. Quantitative InfraRed Thermography Journal 2021. doi: 10.1080/17686733.2021.1918514.

[27] Perez L, Wang J. The effectiveness of data augmentation in image classification using deep learning. Cornell University arXiv 2017. doi: 10.48550/arXiv.1712.04621

[28] Roth HR, Lee CT, Shin HC, Seff A, Kim L et al. Anatomy-specific classification of medical images using deep convolutional nets. In: IEEE 12th International Symposium on Biomedical Imaging (ISBI); New York, NY, USA; 2015. pp. 101 - 104.

[29] Hinton GE, Krizhevsky A, Wang SD. Transforming auto-encoders. In: 21st International Conference on Artificial Neural Networks; Espoo, Finland; 2011. pp. 44-51.

[30] Sabour S, Frosst N, Hinton GE. Dynamic Routing Between Capsules. In: 31st Conference on Neural Information Processing Systems; Long Beach, CA, USA; 2017. pp. 3859–3869.

[31] Shahroudnejad A, Mohammadi A, Plataniotis KN. Improved Explainability of Capsule Networks: Relevance Path by Agreement. In: IEEE Global Conference on Signal and Information Processing (GlobalSIP); Anaheim, CA, USA; 2018. pp. 549-553.

[32] Liu T, Wang Z. HiCNN: a very deep convolutional neural network to better enhance the resolution of Hi-C data. Bioinformatics 2019; 35 (21): 4222-4228. doi: 10.1093/bioinformatics/btz251

[33] He K, Zhang X, Ren S, Sun J. Deep residual learning for image recognition. In: IEEE Conference on Computer Vision and Pattern Recognition (CVPR); Las Vegas, NV, USA; 2016. pp. 770–778.

[34] Szegedy C, Liu W, Jia Y, Sermanet P, Reed S et al. Going Deeper with Convolutions. In: IEEE Conference on Computer Vision and Pattern Recognition (CVPR); Boston, MA, USA; 2015. pp. 1-9.

[35] Ozdemir MA, Ozdemir GD, Guren O. Classification of COVID-19 electrocardiograms by using hexaxial feature mapping and deep learning. BMC Medical Informatics and Decision Making 2021; 21: 170. doi: 10.1186/s12911-021-01521-x.

[36] Kingma DP. Adam: a method for stochastic optimization. Cornell university arXiv 2015. doi: 10.48550/arXiv.1412.6980

[37] Amyar A, Modzelewski R, Li H, Ruan S. Multi-task deep learning based CT imaging analysis for covid-19 pneumonia: classifcation and segmentation. Computers in Biology and Medicine 2020; 126: 104037. doi: 10.1016/j.compbiomed.2020.104037.

[38] Yeung M, Sala E, Schönlieb CB, Leonardo R. Unified Focal loss: Generalising Dice and cross entropy-based losses to handle class imbalanced medical image segmentation. Computerized Medical Imaging and Graphics 2022; 25:102026. doi: 10.1016/j.compmedimag 2021.102026

[39] Ozdemir MA, Degirmenci M, Izci E, Akan A. EEG-based emotion recognition with deep convolutional neural networks. Biomedical Engineering / Biomedizinische Technik 2021; 66 (1): 43–58. doi: 10.1515/bmt-2021-frontmatter1

[40] Li WT, Ma J, Shende N, Castaneda G, Chakladar J et al. Using machine learning of clinical data to diagnose Covid-19: a systematic review and meta-analysis. BMC medical informatics and decision making 2020; 20 (1): 247. doi: 10.1186/s12911-020-01266-z.

[41] Fatourechi M, Ward RK, Mason SG, Huggins J, Schlögl A et al. Comparison of Evaluation Metrics in Classification Applications with Imbalanced Datasets. In: 2008 Seventh International Conference on Machine Learning and Applications; San Diego, CA, USA; 2008. pp. 777-782.

Appendix 1

The main objective of this Appendix 1 was to assess the existing research done in this domain of machine and deep learning application in the classification of breast cancer utilizing the infrared thermal images. For this purpose, popular research databases on the likes of IEEE Xplore and PubMed with the particular search items are searched exhaustively. The research studies included in this appendix are based on the following selection criteria:

1. Only deep learning based approaches for the breast cancer classification using the Infrared thermal images are included.
2. Only machine learning based approaches for the Breast cancer classification using the Infrared thermal images are included.
3. The research studies were limited to the interval from 2016 to October 2021.
4. Only classification or detection approaches are included, whereas prediction approaches utilizing big data are not excluded from this study.
5. The research studies should mention the future direction or at least offer some narrative to improve the existing work are also included.

The table 1 below simply summarize the search items employed for the searching of these unique research studies for the Thermography based Breast cancer classification.

Table 1. The list of research article sources and search items used

Research studies sources	Search terms
IEEE Xplore	"Breast cancer" AND "Deep learning" AND "Infrared thermal images" OR “Thermography” " Breast cancer " AND "CNN" AND “Infrared thermal images" OR “Thermography” " Breast cancer " AND "Deep transfer learning" AND “Infrared thermal images" OR “Thermography” " Breast cancer " AND "ML" AND “Infrared thermal images" OR “Thermography” OR “Thermal images” " Breast cancer " AND "Machine learning" AND “Infrared thermal images" OR “Thermography” OR “Thermal images” filter applied: journals only Publication year: 2016 to 2021
PubMed	" Breast cancer" AND "Deep learning" AND "Infrared thermal images" OR “Thermography” " Breast cancer " AND "CNN" AND "Infrared thermal images" OR “Thermography” " Breast cancer " AND "Deep transfer learning" AND "Infrared thermal images" OR “Thermography” " Breast cancer " AND "Machine learning" AND "Infrared thermal images" OR “Thermography” " Breast cancer " AND "ML" AND "Infrared thermal images" OR “Thermography”

Whereas the Graph 1 below simply presents the search results i.e. paper counts of five years i.e. from 2016 to 2021 illustrating the comparison among the number of research and reviews articles

published related to the Breast cancer classification utilizing the thermography images based on Machine learning and deep learning as per IEEE Xplore and PubMed research databases.

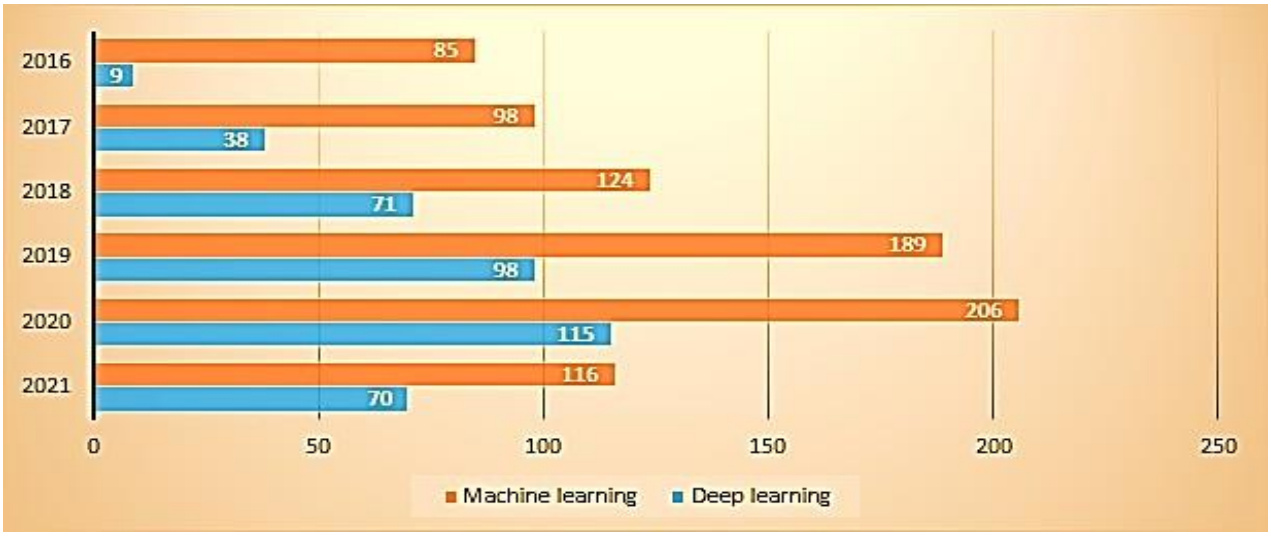

Graph 1. The search results of five years i.e. from 2016 to 2021 illustrating the comparison among the number of research and reviews articles published related to the Breast cancer classification utilizing the thermography images based on Machine learning and deep learning as per IEEE Xplore and PubMed research databases.

A brief comparison among these state of the art Thermography or Infrared thermal images based Breast cancer classification approaches is presented with the aid of table 2 and 3.

Table 2: Comparison among the major state of the art breast cancer classification approaches using thermography based on machine learning

Author and year	**Machine learning classifiers used**	**Thermal image lateral view is used**	**Thermography Acquisition protocol used**	**Results (Accuracy Percentage)**
Silva et al. and 2016 [1]	BayesNet and Radom Forest (RF), KNN classifiers	Frontal view	Dynamic	95.36%
Lashkari et al. and 2016 [2]	AdaBoost, SVM, KNN, NB etc. classifiers	Frontal view	-	AdaBoost = 85.33 % (left breast) AdaBoost = 87.42% (right breast)
Raghavendra et al. and 2016[3]	KNN, Decision Tree (DT), NB, PNN, SVM etc.	Frontal view	-	DT = 98%
Sathish et al. and 2017 [4]	Linear, Polynomial, Gaussian and quadratic SVM classifier	Frontal view	Static	Gaussian SVM = 91%
Gogoi et al. and 2017 [5]	DT, KNN, SVM, NB, ANN, RF, LDA and AdaBoost	Frontal view	Static	SVM = 97.33% (Best) ANN = of 92.5% (Best)

Santana et al. and 2018 [6]	Multilayer Perceptron networks (MLP) and Extreme Learning Machines (ELM)	Left, right and frontal view alone	-	83% (Overall)
Madhavi et al. and 2019 [7]	GLCM, GLSZM, GLRLM, NGTDM along with LSSVM classifier	Left, right and frontal view alone	Static	96%
AlFayez et al. and 2020 [8]	Extreme Learning Machine (ELM) Classifier and Multilayer Perceptron (MLP) Classifier	Frontal view only	Static	ELM = 100% MLP = 82.2%
Mishra et al. and 2020 [9]	GLCM, GLRL along with RF, KNN etc.	Frontal view only	Static	RF=95.45%
Karthiga et al. and 2021 [10]	Logistic regression(LR), Linear SVM, Quadratic SVM, Cubic SVM, Fine Gaussian SVM, Medium Gaussian SVM, KNN etc.	Frontal view only	Static and Dynamic	SVM = 93.3%.

Table 3: Comparison among the major state of the art Breast cancer classification approaches using Thermography based on Deep learning

Author and year	**Which model is used**	**Which Thermal image lateral view is used**	**Thermography Acquisition protocol used**	**Results (Accuracy Percentage)**
Roslidar et al. and 2019[11]	ResNet101, ShuffleNetV2, DenseNet and MobileNetV2	Frontal view only	Static and Dynamic	DenseNet201 = 100%
Fernández-vies et al. and 2019 [12]	ResNet18, ResNet34, ResNet50, ResNet152, VGG16 and VGG19	Frontal view only	Static	Resnet50 = 98.65%
Yadav et al. and 2020[13]	Augmentation method along with Baseline CNN Model, VGG16, InceptionV3	Frontal view only	-	Inception V3 = 98.5%
Ekici et al. and 2020 [14]	Convolutional neural networks optimized by Bayes algorithm	Left, Right and Frontal alone	Static and Dynamic	98.95%
Galván et al. and 2021 [15]	ResNet-101	Frontal view only	Static	ResNet-101 delivers sensitivity of 92.3% and specificity of 53.8%

References

[1] L.F. Silva, A.A.S. Santos, R.S. Bravo, A.C. Silva, D.C. Muchaluat-Saade, A. Conci, Hybrid analysis for indicating patients with breast cancer using temperature time series, Computer Methods Programs Biomed. 130 (2016) 142–153.

[2] A. Lashkari, F. Pak, M. Firouzmand, Full Intelligent Cancer Classification of Thermal Breast Images to Assist Physician in Clinical Diagnostic Applications, J. Med. Signals Sens. 6(1) (2016) 12-24.

[3] U. Raghavendra, U.R. Acharya, E.Y.K Ng, J.H. Tan, A. Gudigar, An integrated index for breast cancer identification using histogram of oriented gradient and kernel locality preserving projection features extracted from Thermal images, Quant. Infr. Thermography J. 13 (2016) 195-209.

[4] D. Sathish, S. Kamath, K. Prasad, R. Kadavigere, Role of normalization of breast Thermal images and automatic classification of breast cancer, Visual Computer 35 (2017) 57-70.

[5] U.R. Gogoi, M.K. Bhowmik, D. Bhattacharjee, A.K. Ghosh, Singular value based characterization and analysis of Thermal patches for early breast abnormality detection, Australasian Physical & Engineering Sciences in Medicine (2018). doi: https://doi.org/10.1007/s13246-018-0681-4.

[6] M.A. Santana, J.M.S. Pereira, F.L. Silva, N.M. Lima, F.N. Sousa, G.M.S. Arruda, W.P. Santos, Breast cancer diagnosis based on mammary thermography and extreme learning machines, Research on Biomedical Engineering 34(1), 45–53 (2018).

[7] Madhavi, V., Thomas, C.B.: Multi-view breast Thermal images analysis by fusing texture features. Quantitative InfraRed Thermography Journal, 16(1), 111–128 (2019). doi:10.1080/17686733.2018.1544687.

[8] AlFayez, F., El-Soud, M.W.A., Gaber, T.: Thermal images Breast Cancer Detection: A Comparative Study of Two Machine Learning Techniques. Applied Sciences 10(2), 551 (2020).

[9] V. Mishra, S.K. Rath, Detection of breast cancer tumours based on feature reduction and classification of Thermal images, Quantitative InfraRed Thermography Journal (2021). doi:10.1080/17686733.2020.1768497.

[10] R. Karthiga, K. Narasimhan, Medical imaging technique using curvelet transform and machine learning for the automated diagnosis of breast cancer from Thermal image, Pattern Anal. Application (2021). doi:https://doi.org/10.1007/s10044-021-00963-3.

[11] R. Roslidar, K. Saddami, F. Arnia, M. Syukri, K. Munadi, A study of fine-tuning CNN models based on Thermal imaging for breast cancer classification, In: Proceedings of IEEE Int. Conf. Cybern. Comput. Intell. (CyberneticsCom) 77-81 (2019).

[12] F.J. Fernández-Ovies, E.S.de. Alférez-Baquero, E.J. Andrés-galiana, Detection of breast cancer using infrared thermography and deep neural networks, In: International Work-Conference on Bioinformatics and Biomedical Engineering, Granada, Spain 514–523 (2019).

[13] S.S. Yadav, S.M. Jadhav, Thermal infrared imaging based breast cancer diagnosis using machine learning techniques, Multimedia Tools and Applications (2020). doi: https://doi.org/10.1007/s11042-020-09600-3.

[14] S. Ekici, H. Jawzal, Breast cancer diagnosis using thermography and convolutional neural networks. Medical Hypotheses 137 (2020). doi: https://doi.org/10.1016/j.mehy.2019.109542.

[15] Galv´an JCT, Guevara E, Machuca EMK, Villanueva AC, Flores JL, Gonza´lez FJ. Deep convolutional neural 25 networks for classifying breast cancer using infrared thermography. Quantitative InfraRed Thermography Journal 26 2021. doi: https://doi.org/10.1080/17686733.2021.1918514.

Appendix 2

Layer (type)	Output Shape	Param #
input_12 (InputLayer)	[(None, 480, 120, 3)]	0
Conv1 (Conv2D)	(None, 472, 112, 256)	62464
primarycap_conv2d (Conv2D)	(None, 232, 52, 256)	5308672
primarycap_reshape (Reshape)	(None, 386048, 8)	0
primarycap_squash (Lambda)	(None, 386048, 8)	0
digitcaps(CapsuleLayer)	(None, 2, 16)	98828288
capsnet (Length)	(None, 2)	0
Total params: 104,199,424		
Trainable params: 104,199,424		
Non-trainable params: 0		

Table 1: The proposed capsule network model summary for the breast cancer detection utilizing the infrared thermal images.

Appendix 3

The confusion matrices of the proposed "Breast Cancer-Caps" system over the test Static and Dynamic breast thermal images datasets consisting of the 25 breast cancer and 25 normal breast thermal images for each views i.e. multiview, left, right and frontal are presented with the aid of figures below. In these confusion matrices, true positive means a breast thermal image belongs to a patient diagnosed with breast cancer and the proposed system correctly classified this breast thermal image as breast cancer or abnormal image. On the other hand, the false positive means a breast thermal image belongs to a patient diagnosed with breast cancer and the proposed system incorrectly classified this breast thermal image as a normal image. Whereas the true negative means a breast thermal image belongs to a healthy or normal patient and the proposed system correctly classified this breast thermal image as a normal image. Finally the false negative means a breast thermal image belongs to a healthy or normal patient and the proposed system incorrectly classified this breast thermal image as an abnormal image.

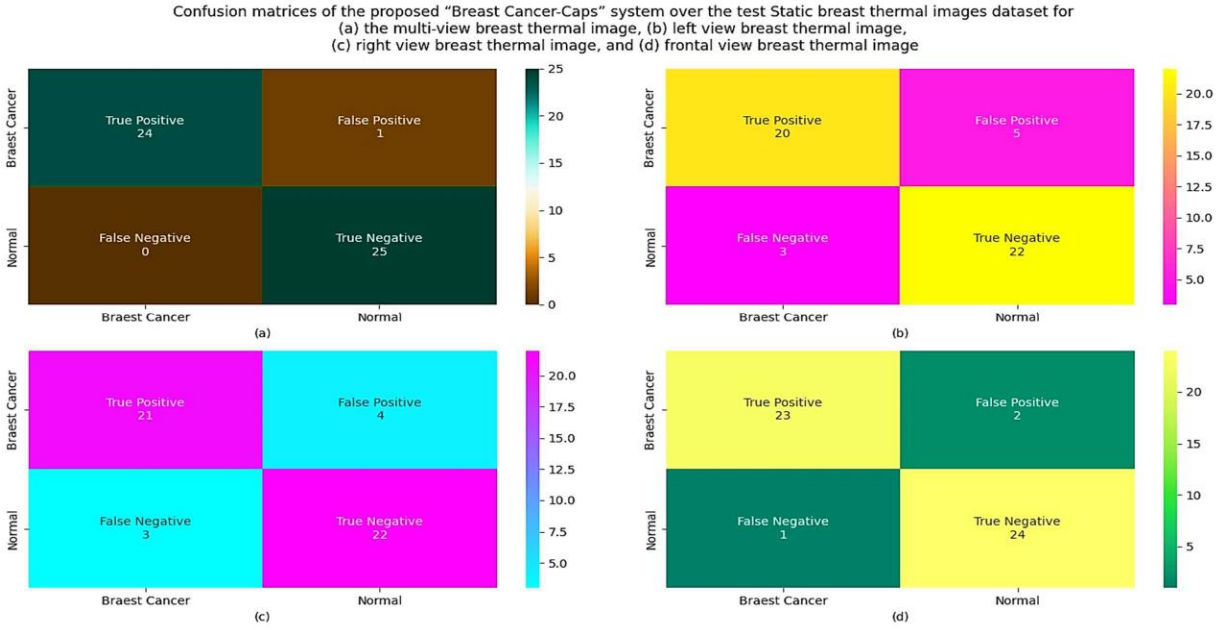

Confusion matrices of the proposed "Breast Cancer-Caps" system over the test Dynamic breast thermal images dataset for (a) the multi-view breast thermal image, (b) left view breast thermal image, (c) right view breast thermal image, and (d) frontal view breast thermal image

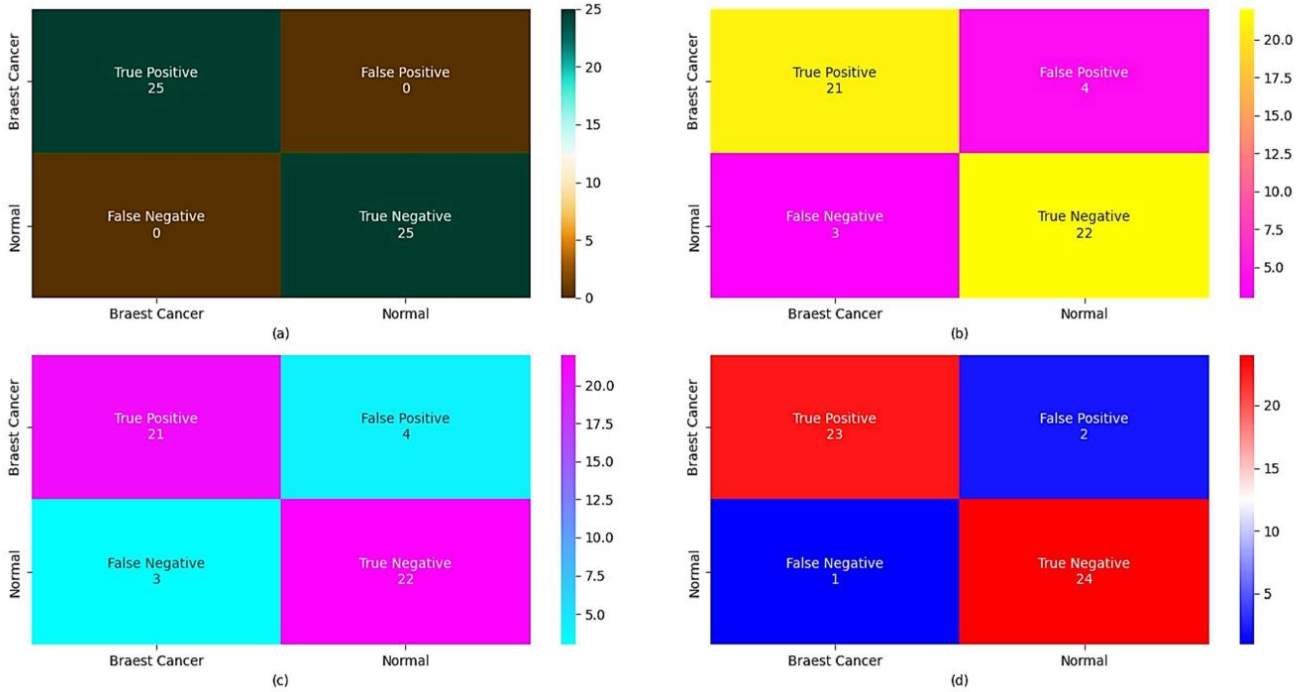

Similarly the confusion matrices of the systems used for comparison based on VGG19, ResNet50 and InceptionV3 models over the test Static and Dynamic breast thermal images datasets consisting of the 25 breast cancer and 25 normal breast thermal images for each views i.e. multiview, left, right and frontal are presented with the aid of figures below.

Confusion matrices of the system based on VGG19 model used for the comparison over the test Static breast thermal images dataset for (a) the multi-view breast thermal image, (b) left view breast thermal image, (c) right view breast thermal image, and (d) frontal view breast thermal image

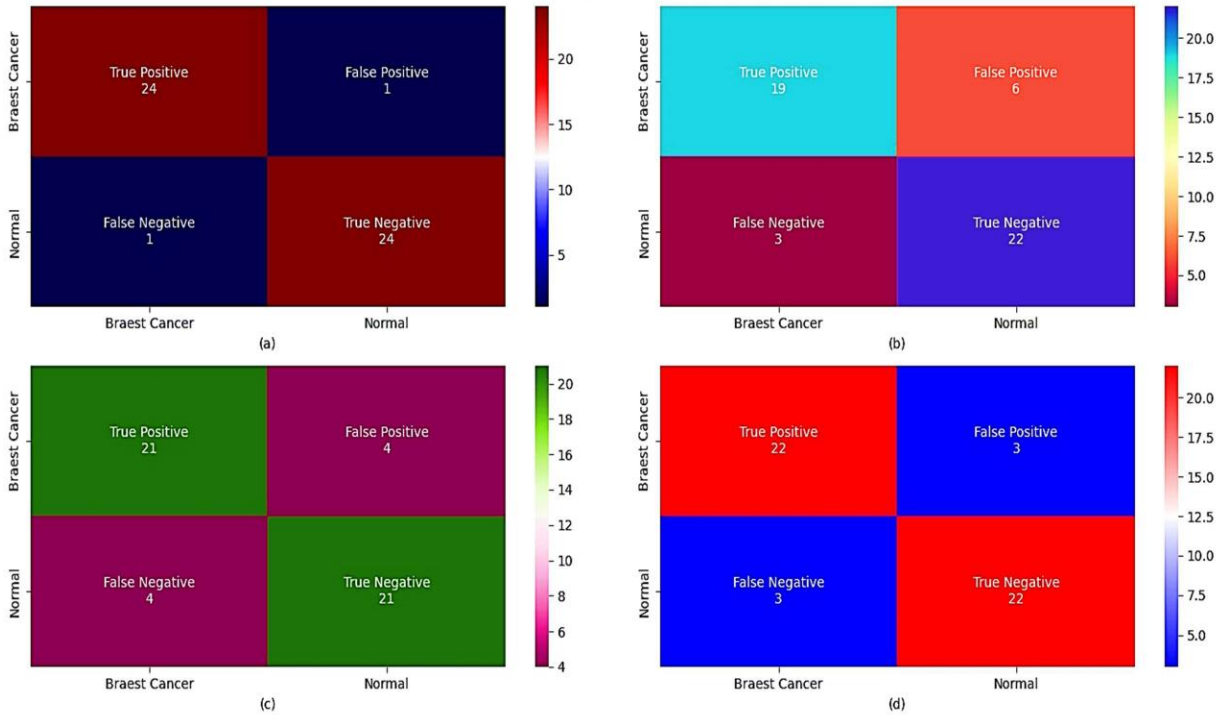

Confusion matrices of the system based on VGG19 model used for the comparison over the test Dynamic breast thermal images dataset for (a) the multi-view breast thermal image, (b) left view breast thermal image, (c) right view breast thermal image, and (d) frontal view breast thermal image

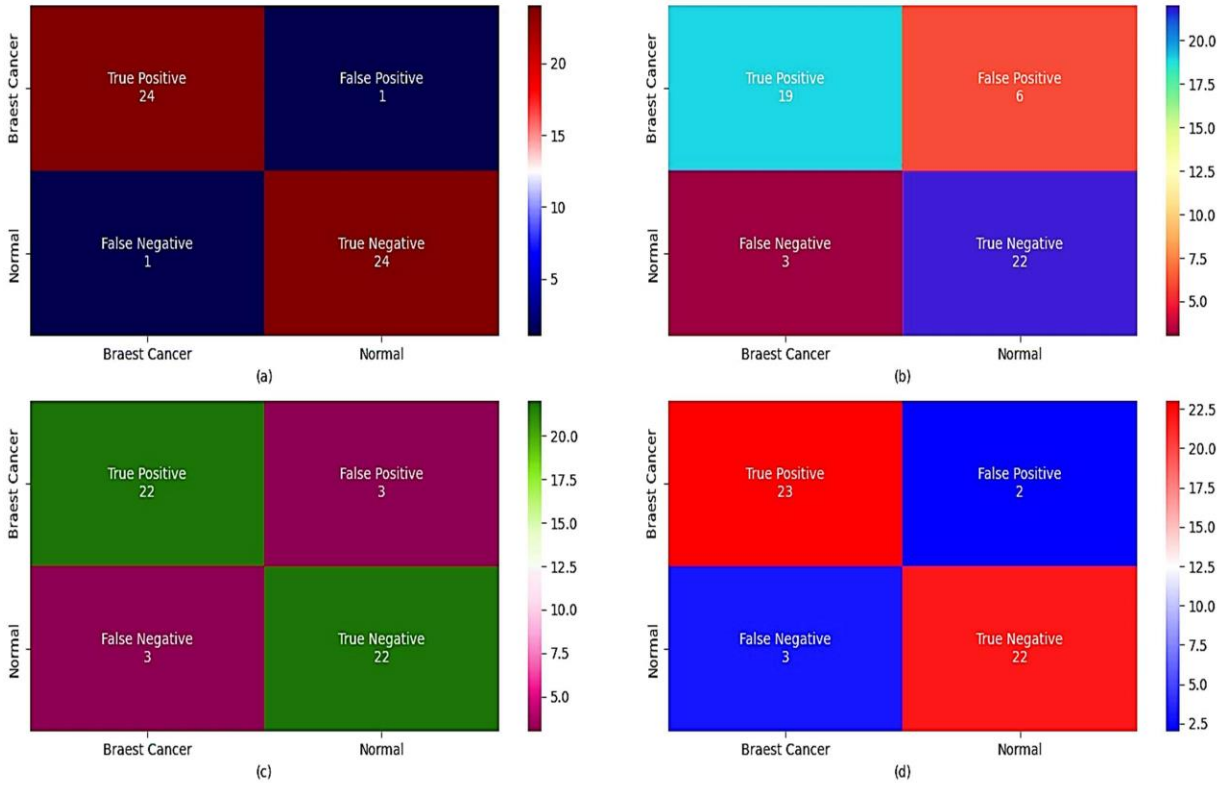

Confusion matrices of the system based on ResNet50 model used for the comparison over the test Static breast thermal images dataset for (a) the multi-view breast thermal image, (b) left view breast thermal image, (c) right view breast thermal image, and (d) frontal view breast thermal image

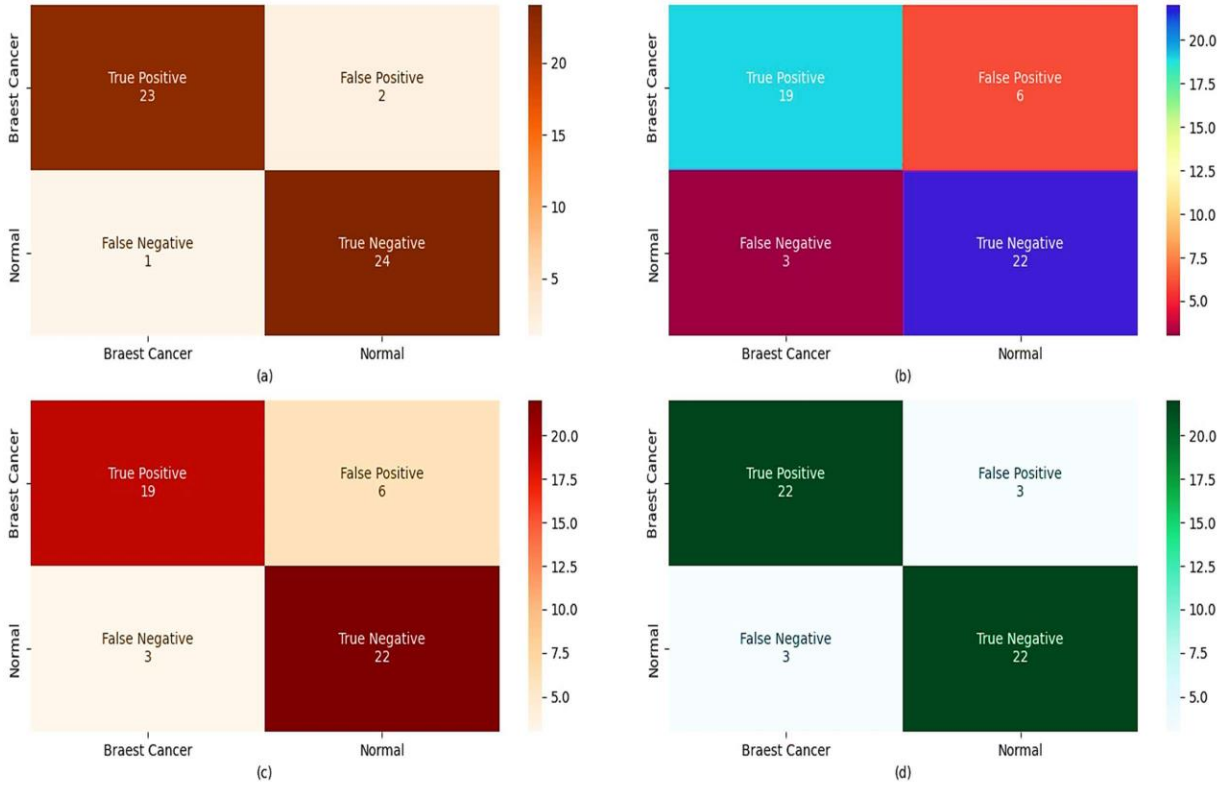

Confusion matrices of the system based on ResNet50 model used for the comparison over the test Dynamic breast thermal images dataset for (a) the multi-view breast thermal image, (b) left view breast thermal image, (c) right view breast thermal image, and (d) frontal view breast thermal image

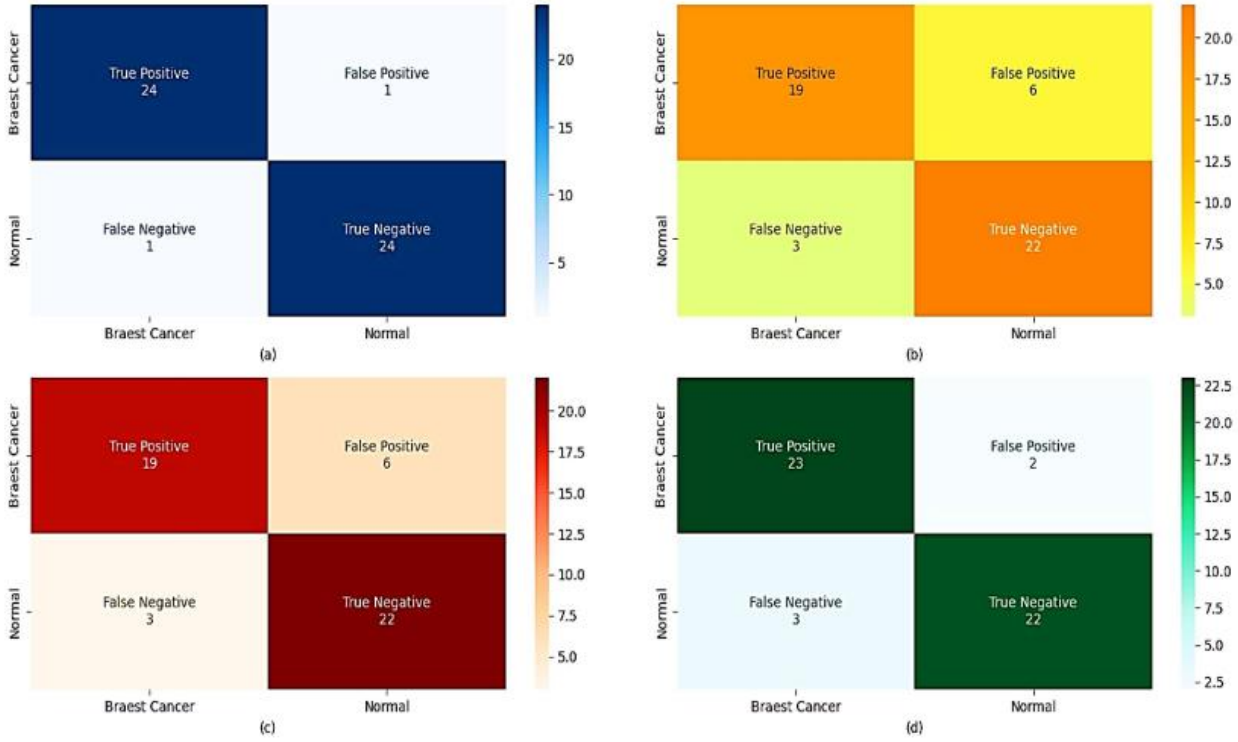

Confusion matrices of the system based on InceptionV3 model used for the comparison over the test Static breast thermal images dataset for (a) the multi-view breast thermal image, (b) left view breast thermal image, (c) right view breast thermal image, and (d) frontal view breast thermal image

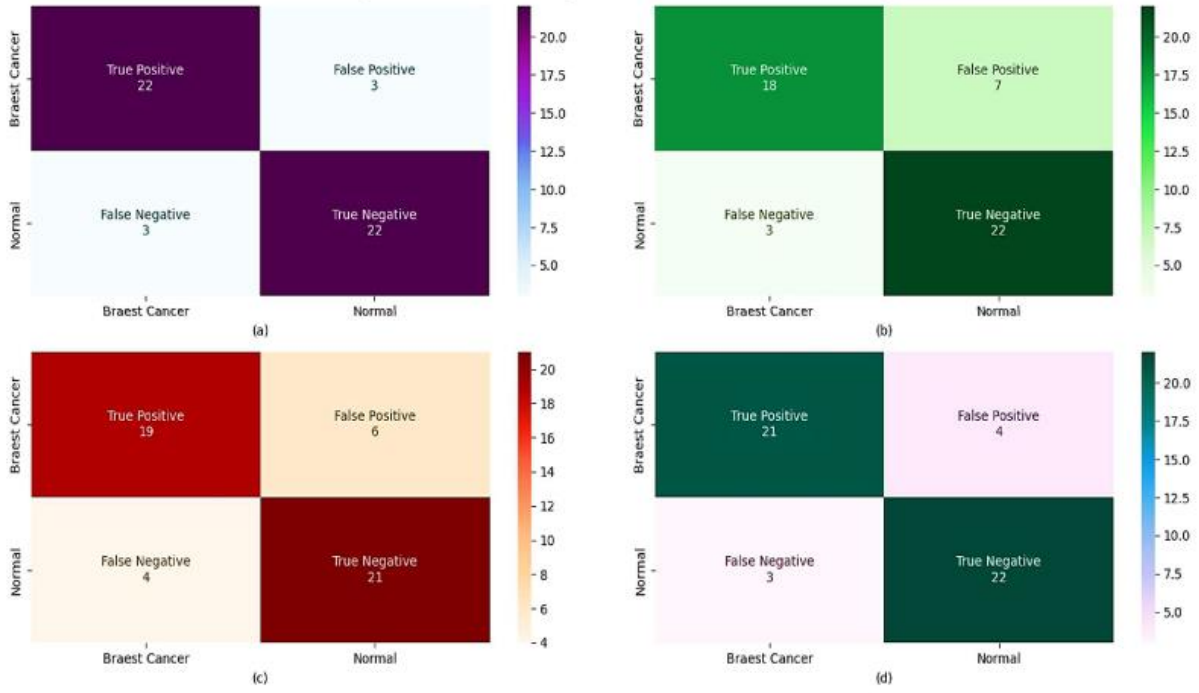

Confusion matrices of the system based on InceptionV3 model used for the comparison over the test Dynamic breast thermal images dataset for (a) the multi-view breast thermal image, (b) left view breast thermal image, (c) right view breast thermal image, and (d) frontal view breast thermal image

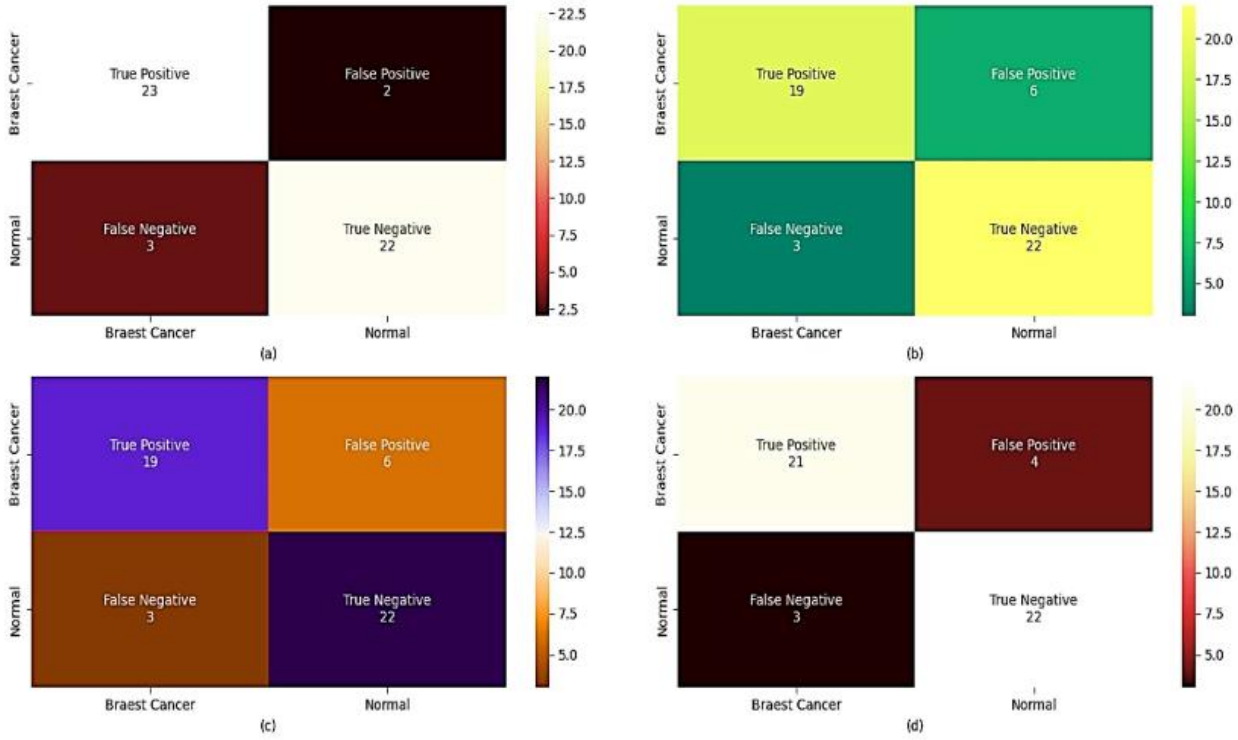

Table 1 Performance comparison of the Proposed "Breast Cancer-Caps" system with the existing deep learning based state of the art approaches for the breast cancer classification over the Static breast thermal images testing dataset

Author and year	Breast view	Accuracy	Precision	Sensitivity	Specificity	F1 score	MSE	LOSS	AUC	Kappa
Fernández-vies et al. and 2019 [1]	Multi	94	94	94	94	94	0.07	0.448	97.1	0.88
	Left	81	82	80.3	81.6	81.1	0.184	0.69	89.9	0.61
	Right	82	80	83.3	80.7	81.6	0.181	0.68	90.2	0.62
	Frontal	90	84	95.4	85.7	89.3	0.147	0.418	92.8	0.80
Yadav et al. and 2020[2]	Multi	89	88	89.8	88.24	88.9	0.148	0.438	92.7	0.76
	Left	80	76	82.6	77.7	79.17	0.187	0.695	89.2	0.6
	Right	81	78	82.9	79.2	80.4	0.184	0.69	89.9	0.61
	Frontal	84	78	88.6	80.3	82.9	0.175	0.64	90.8	0.65
Proposed Breast Cancer-Caps system	**Multi**	**98**	**98**	**98**	**98**	**98**	**0.021**	**0.086**	**98.2**	**0.96**
	Left	**83**	**84**	**82.3**	**83.6**	**83**	**0.178**	**0.66**	**90.5**	**0.68**
	Right	**87**	**86**	**87**	**86.2**	**86**	**0.151**	**0.340**	**92.5**	**0.72**
	Frontal	**93**	**90**	**95**	**92**	**92**	**0.071**	**0.151**	**96.5**	**0.88**

Table 2 Performance comparison of the Proposed "Breast Cancer-Caps" system with the existing deep learning based state of the art approaches for the breast cancer classification over the Dynamic breast thermal images testing dataset

Author and year	Breast view	Accuracy	Precision	Sensitivity	Specificity	F1 score	MSE	LOSS	AUC	Kappa
Fernández-vies et al. and 2019 [1]	Multi	95	96	94.12	95.9	95	0.068	0.452	96.7	0.96
	Left	82	82	82	82	82	0.181	0.68	89.5	0.64
	Right	83	82	83.6	82.3	82.8	0.178	0.66	90.5	0.64
	Frontal	91	88	93.6	88.68	90.7	0.145	0.411	92.9	0.82
Yadav et al. and 2020[2]	Multi	91	90	91.8	90.2	91	0.145	0.411	92.9	0.82
	Left	82	78	84.7	79.6	81.2	0.179	0.67	90.1	0.64
	Right	83	78	86.6	80	82.1	0.178	0.66	90.5	0.64
	Frontal	85	80	88.8	81.8	84.2	0.174	0.64	91.4	0.65
Proposed Breast Cancer-Caps system	**Multi**	**99.5**	**98.04**	**100**	**100**	**99.01**	**0.019**	**0.084**	**99.1**	**1**
	Left	**85**	**86**	**84.3**	**85.7**	**85.5**	**0.174**	**0.640**	**91.4**	**0.72**
	Right	**87**	**88**	**86.2**	**87.7**	**87.1**	**0.150**	**0.338**	**92.7**	**0.73**
	Frontal	**94**	**92**	**95.8**	**92.31**	**93.88**	**0.070**	**0.148**	**97.1**	**0.88**

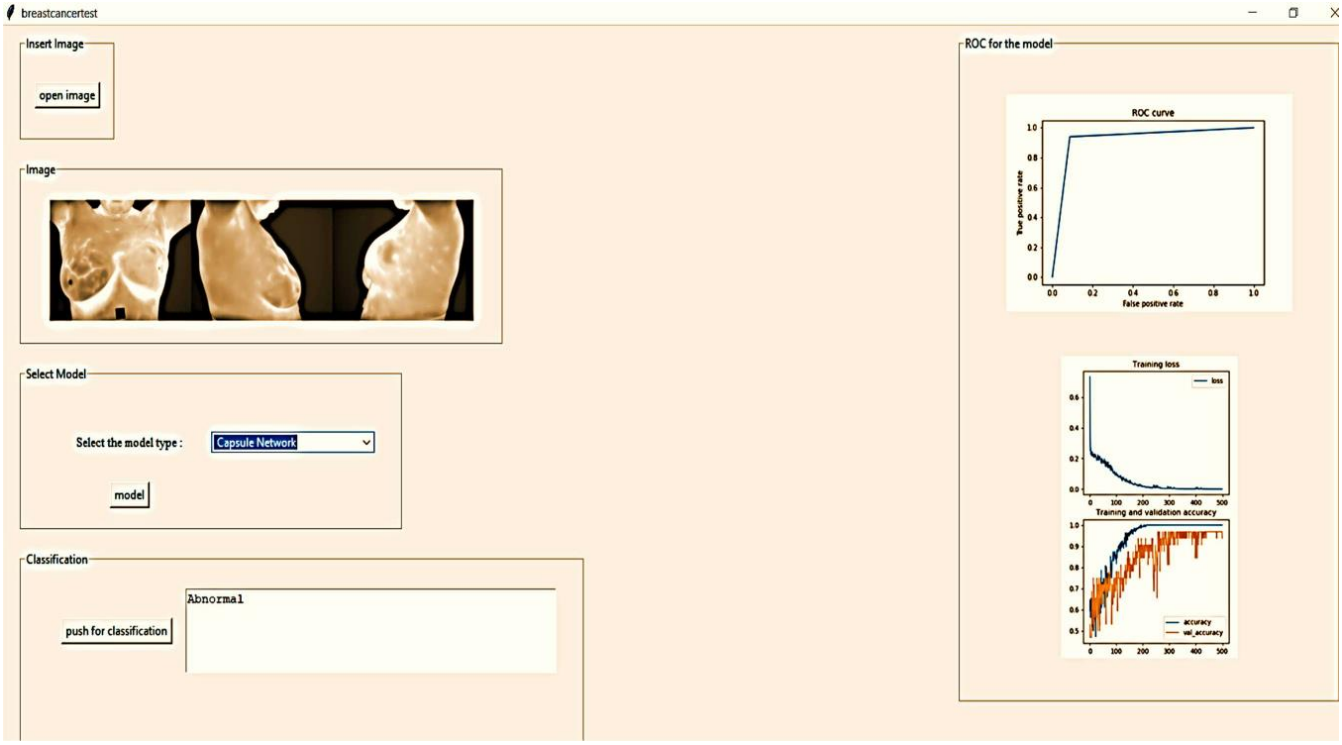

Figure 1: GUI screenshot of the working “Breast Cancer-Caps” early screening system

References

[1] F.J. Fernández-Ovies, E.S.de. Alférez-Baquero, E.J. Andrés-galiana, Detection of breast cancer using infrared thermography and deep neural networks, In: International Work-Conference on Bioinformatics and Biomedical Engineering, Granada, Spain 514–523 (2019).

[2] S.S. Yadav, S.M. Jadhav, Thermal infrared imaging based breast cancer diagnosis using machine learning techniques, Multimedia Tools and Applications (2020). doi: https://doi.org/10.1007/s11042-020-09600-3.